Raman spectrum in $PbTiO_3$ re-examined: dynamics of the soft phonon and the central peak

1991 J. Phys.: Condens. Matter 3 8695

(http://iopscience.iop.org/0953-8984/3/44/014)

J. Phys.: Condens. Matter 3 (1991) 8695–8705. Printed in the UK

Raman spectrum in $PbTiO_3$ re-examined: dynamics of the soft phonon and the central peak

M D Fontana†, H Idrissi†, G E Kugel† and K Wojcik‡

† Centre Lorrain d'Optique et Electronique des Solides, University of Metz and Supelec, 2 rue E Belin, 57078 Metz Cédex 3, France

‡ Institute of Physics, Silesian University, Universitecka 4, 4007 Katowice, Poland

Received 26 April 1991, in final form 11 June 1991

Abstract. Light scattering measurements are investigated as a function of temperature from 10 to 900 K in the tetragonal and cubic phases of a $PbTiO_3$ crystal. Phonon frequencies, ionic effective charges, spontaneous polarization and contribution to the dielectric permittivity are deduced from these data. The results show that the soft phonon and relaxation mode are both needed to describe the dynamics of this material.

1. Introduction

The oxidic perovskites are of current interest in the field of lattice dynamics and structural phase transitions. Among them, $BaTiO_3$, $KNbO_3$, $SrTiO_3$ and $KTaO_3$ have been widely investigated by various experimental techniques. For a long time, the dynamics of the phase transitions in these compounds were thought to be governed by the soft phonon only. The failure of the LST relationship to reproduce the experimental dielectric data [1, 2] as well as the incomplete phonon softening led us to assume the existence of a relaxation process at frequencies below the soft phonon and thus a more complicated mechanism for the phase transitions. This relaxation mode was confirmed by the appearance of a central peak in the light scattering experiments [3] and/or the appearance of a dielectric radio-frequency dispersion [4] in the vicinity of phase transition. A predominant order–disorder mechanism is therefore now used to describe the phase transitions in $KNbO_3$, $BaTiO_3$ and $KTa_{1-x}Nb_xO_3$ (KTN).

Since a disorder process is also invoked to play a role in the phase transitions in $AgNbO_3$ [5], $PbZrO_3$, $Pb(Zr, Ti)O_3$ [6], $LiNbO_3$ and $LiTaO_3$ [7], lead titanate $PbTiO_3$ appears up to very recently the sole oxidic perovskite the dynamics of which could be described by the classical Cochran–Anderson theory. Lattice modes in $PbTiO_3$ were studied by inelastic neutron scattering in the cubic and tetragonal phases [8] and by Raman measurements in the tetragonal phase [9, 10]. Results reveal the softening of the lowest-frequency transverse optical (TO) modes of E and A_1 symmetry when T_c ($\simeq$495 °C) is approached. These soft modes are underdamped even in the close vicinity of T_c. From the above discussion on the mechanism of the phase transitions in ABO_3 compounds, the following remarks can be made concerning $PbTiO_3$.

(i) The soft-mode frequency does not go to zero at T_c but saturates at around 50 cm^{-1}.

0953-8984/91/448695 + 11 $03.50

(ii) The possible presence of an additional peak below phonon frequencies was not found in the previous Raman measurements [9, 10] which were limited down to 15 cm^{-1} from the laser line.

(iii) The comparison between experimental dielectric data and the values calculated from phonon frequencies via the LST relationship was never attempted as a function of temperature.

In order to clarify these points, new Raman investigations of $PbTiO_3$ are needed in the tetragonal phase from room temperature up to T_c with a particular care to measurements for small frequency shifts and for the vicinity of T_c.

Two additional features merit attention and justifies the extension of Raman measurements also below room temperature and above T_c. First, the existence of one or two supplementary phase transitions at low temperatures was deduced from dielectric and x-ray investigations [11]. It would be interesting to confirm this feature by Raman measurements on a single crystal. The last point concerns the Raman spectrum in the cubic phase which can provide information about lattice dynamics. Indeed the Raman spectrum in the cubic phase of these oxidic ABO_3 compounds is generally characterized by intense second-order scattering [12], which was attributed to the large polarizability of the oxygen ion. This polarizability which is non-linear and anisotropic was found to be responsible for the phonon softening when approaching T_c. It has proved to be dynamically enhanced by the B ion (Ti, Ta or Nb) [12].

A complete study of the Raman spectrum in $PbTiO_3$ is therefore reported in this paper. Measurements are made as a function of the temperature from 10 to 900 K, for various configurations. The results which are obtained are compared with previous investigations as well as with Raman spectra recorded in other oxidic perovskites. The very low-frequency scattered profile is discussed with regard to the possible existence of a central peak, in connection with the dielectric data. The phonon frequencies obtained from Raman data are used to calculate the ionic effective charges, and thus the spontaneous polarization in the tetragonal phase.

2. Experimental results

Raman scattering measurements have been performed on $PbTiO_3$ single crystals prepared by the flux-grown technique [13]. These crystals with a typical 2 mm × 2 mm × 0.3 mm size possess a relatively low conductivity, which has allowed us to make dielectric measurements on the same sample as used for Raman experiments. Raman data are taken with a double Spex monochromator using a 633 nm He–Ne laser beam.

In the tetragonal phase (C_{4v}^1 space group) the optical lattice modes transform as $3A_1 + 4E + B_1$ species. All these modes are first-order Raman active and all but B_1 are infrared active. According to the compatibility relations between the cubic and the tetragonal modes the three $A_1 + E$ phonons arise from the three F_{1u} modes of the cubic phase whereas one E mode and the B_1 mode come from the F_{2u} silent (infrared-inactive) mode.

We choose the sample geometry with the tetragonal *c* axis normal to the scattered plane so that the simultaneous observation of the A_1 and E optical modes can be achieved in the same experimental conditions.

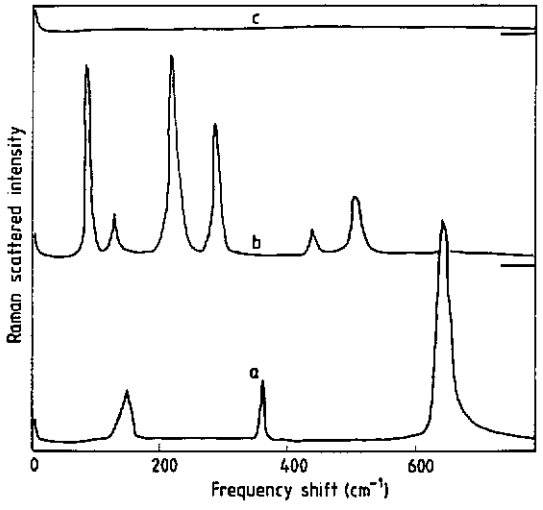

Figure 1. Raman spectra in tetragonal $PbTiO_3$ at room temperature. The spectra denoted a, b and c correspond to the $X(ZZ)Y$, $X(ZX)Y$ and $X(YX)Y$ scattering geometries, respectively, and are recorded in the same experimental conditions.

2.1. Raman spectra at room temperature and low temperatures

The results obtained at room temperature are given in figure 1. The $X(ZZ)Y$ spectrum, denoted spectrum a, gives rise to the A_1(TO) lines whereas the $X(ZX)Y$ (or the $X(YZ)Y$) spectrum, denoted spectrum b, allows the simultaneous detection of the E(TO) and E(LO) phonons. The $X(YX)Y$ spectrum (spectrum c) corresponds to extinction since no phonon mode is in principle expected in this configuration. The spectrum a exhibits two small lines located at 148 cm^{-1} and 362 cm^{-1} and a very intense peak at 650 cm^{-1}. These lines are attributed to the phonons A_1(TO1), A_1(TO2) and A_1(TO3), respectively. Spectrum b displays lines lying at 89 cm^{-1}, 220 cm^{-1} and 508 cm^{-1} which are due to the phonons E(TO1), E(TO2) and E(TO3), respectively. The peaks at around 130 cm^{-1} and 440 cm^{-1} correspond to E(LO1) and E(LO2) phonons whereas a weak band around 720 cm^{-1} (not visible in the figure) can be assigned to the E(LO3) phonon. Finally, the intense line at 290 cm^{-1} is due to the E(TO4–LO4) phonon from the non-polar F_{2u} cubic mode. No line is detected in spectrum c, in agreement with the symmetry requirements. This fact as well as the clear light polarization effect that is observed between spectra a and b prove the excellent optical quality and the single-domain character of the $PbTiO_3$ sample used in our experiments. This allows quantitative comparison in the temperature behaviour between the A_1 and E modes as well as study of the low-frequency scattering which has to be intrinsic. Further, for each temperature, spectrum c is used as the reference scattering arising from crystal imperfections and various noise sources. Our results at room temperature agree well with those of previous investigations [9, 10] except for the lowest A_1(TO1) line at 148 cm^{-1} for which a contradiction can be seen. Indeed the lowest peak in spectrum a was interpreted as an extraneous line by Burns and Dacoll [9]. In our results we exclude the possibility of contamination from another symmetry and we assign this line to an A_1(TO) phonon.

The E and A_1 spectra in tetragonal $PbTiO_3$ can be compared with analogous spectra recorded in isomorphous $BaTiO_3$ [1]. Several differences can be observed. In $PbTiO_3$

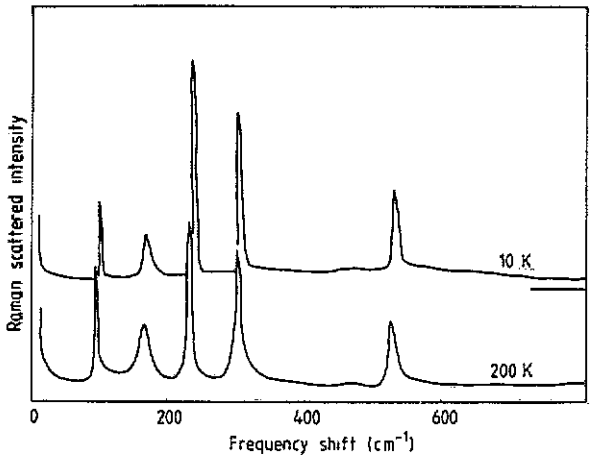

Figure 2. E-type phonon spectrum at two different temperatures (200 and 10 K).

the two lowest A_1 lines display an intensity much weaker than the corresponding E peaks, contrary to $BaTiO_3$. Further, the second line E(TO2) presents an intensity comparable with that of the first line E(TO1), while it is much less intense in $BaTiO_3$, $KNbO_3$ and KTN. A tentative explanation for this will be given below.

Now we examine the possibility of the occurrence of phase transitions at low temperatures by measuring the Raman spectrum from 300 down to 10 K. We do not observe a line coalescence or disappearance as in a ferrodistortive phase transition, nor do we see an onset of new lines activated by a zone boundary folding as in an antidistortive transition. Thus, spectrum b recorded at 200 and 10 K and given in figure 2 does not display a qualitative change indicative of a structural transformation. Only a slight and continuous frequency increase of the lines is detected when the temperature decreases. Our Raman data consequently do not favour the existence of any phase transition at low temperatures. This feature is in contrast with isostructural compounds such as $BaTiO_3$ and $KNbO_3$ which undergo, in addition to the cubic-to-tetragonal transition, the tetragonal-to-orthorhombic-to-rhombohedral transformation.

2.2. Raman spectra at high temperatures

Spectra a, b and c are studied at high temperatures with particular attention devoted to the low-frequency spectrum. For this, the good optical quality of the $PbTiO_3$ sample as well as the spectrometer resolution allow measurement of the light scattered intensity down to 2 cm^{-1} from the Rayleigh line. The lowest A_1(TO1) and E(TO1) lines shift downwards continuously when the temperature increases from 20 to 495 °C and then abruptly disappear in the cubic phase like any first-order line. This result, which is illustrated in figures 3 and 4, is in agreement with the previous Raman investigations [9, 10]. Nevertheless the surprising feature revealed by our data consists of the occurrence of quasi-elastic scattering in spectrum b above 430 °C, as shown in figure 5. This scattering intensity grows when T_c is approached from below, then decreases above T_c in the cubic phase and finally vanishes above 600 °C.

The intrinsic origin of this quasi-elastic scattering can be questioned. This scattering is anisotropic in the tetragonal phase since it does not occur in spectra a and c. It cannot

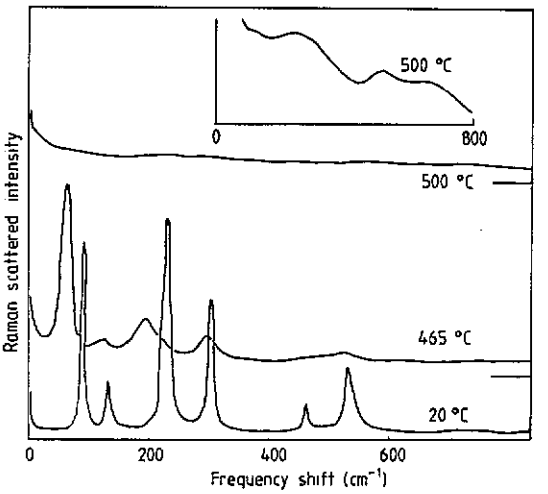

Figure 3. E-type spectrum recorded in the same experimental conditions at various temperatures in the tetragonal (20 and 465 °C) and the cubic (500 °C) phases. The inset shows this same spectrum at 500 °C when the entrance slit width of the spectrometer is much larger (500 μm instead of 200 μm).

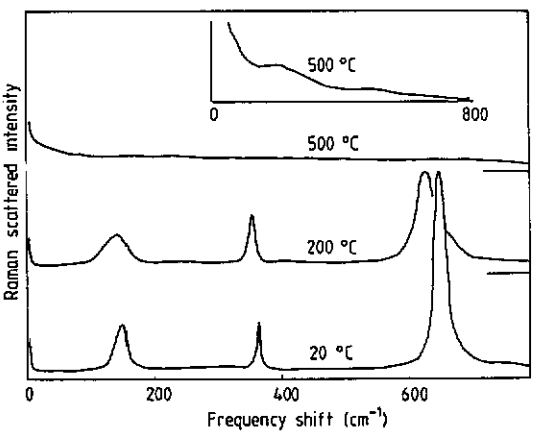

Figure 4. A_1(TO)-type spectrum recorded at 20 and 200 °C in the tetragonal phase and at 500 °C in the cubic phase. The inset shows the cubic spectrum with the entrance slit width of the spectrometer equal to 500 μm instead of 200 μm.

therefore be attributed to crystal imperfections. The presence of domains is also excluded since the selection rules are perfectly obeyed in the recorded Raman spectra. The quasi-elastic scattering, which has the same symmetry as the E phonon lines, consequently seems to have a dynamic origin. Since it displays the well known central peak behaviour as a function of temperature, it is apparently closely related to the phase transition mechanism.

As long as the experimental conditions are the same as in the tetragonal phase, the Raman spectra in the cubic phase exhibit solely the quasi-elastic scattering. The second-order bands expected as a result of the cubic symmetry are visible only if the spectrometer

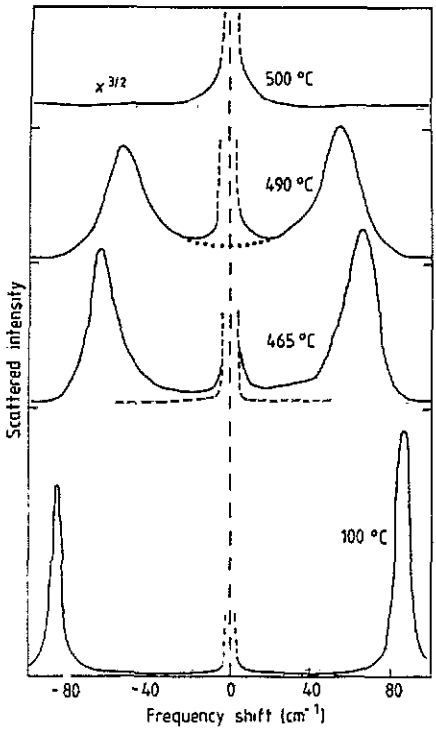

Figure 5. Low-frequency E spectrum at various temperatures. The broken curve in the spectrum at 465 °C is the Rayleigh line contribution recorded in the $X(YX)Y$ configuration. The dotted curve in the spectrum at 490 °C corresponds to the calculated contribution of the soft phonon at very low frequencies.

slits are opened wide. Figures 3 and 4 show cubic spectra a and b recorded at two different spectrometer resolutions. The magnitude of the second-order scattering is seen to be very weak with respect to the quasi-elastic scattering and therefore with respect to the first-order lines of the tetragonal phase which abruptly disappear above T_c. This feature is completely opposite to the situation occurring in the other cubic oxidic perovskites for which two-phonon scattering is large. This suggests that the oxygen polarizability which is invoked as responsible for the strong second-order Raman processes in $BaTiO_3$, $KNbO_3$ and KTN plays a minor role in the dynamics of $PbTiO_3$. This is corroborated by our recent lattice dynamics calculations described below.

3. Interpretation

3.1. Analysis of the Raman spectra

The phonon lines are analysed in the framework of the usual damped-harmonic-oscillator model. The scattered intensity due to a TOj phonon is therefore adjusted to

$$I(\omega) = KS_j\omega_{TOj}^2/[(\omega_{TOj}^2 - \omega^2)^2 + \omega^2\gamma_{TOj}^2] \tag{1}$$

where S_j, ω_{TOj} and γ_{TOj}, respectively, are the oscillator strength, the frequency and the damping of the jth TO phonon and K is a factor related with the experimental conditions. The frequency and damping of the E(TO1) and A_1(TO1) phonons are thus determined as a function of temperature and reported in figure 6. The results do not significantly

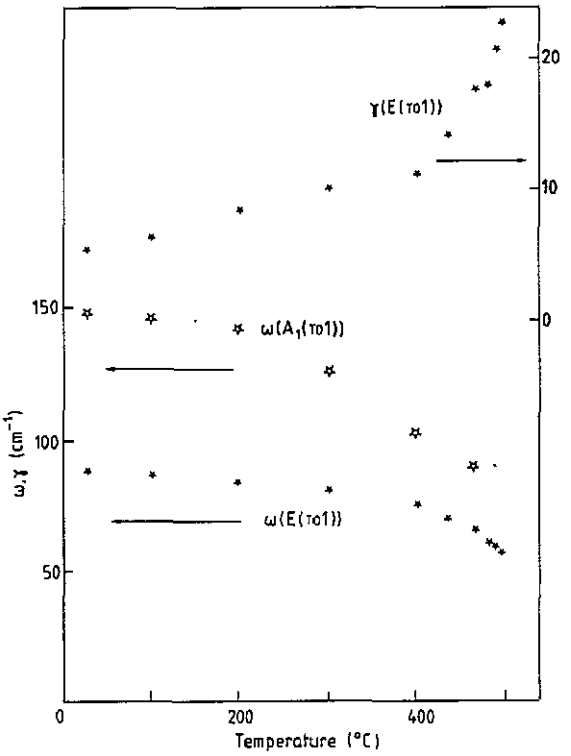

Figure 6. *Temperature dependence of the* E(TO1) frequency, A_1(TO1) frequency and E(TO1) damping, as deduced from fits to Raman data.

differ from those previously reported [9] except for the A_1(TO) mode frequency. Concerning the E(TO1) mode it can be noted that its frequency decreases slowly on heating to 400 °C and then more rapidly up to T_c. Its corresponding damping displays a change in the slope as a function of temperature around the same value (400–420 °C).

The value of the oscillator strength involved in equation (1) is calculated for each TO mode via the relation

$$S_j = \varepsilon(\infty)\omega^{-2}(\mathrm{TO}j)\prod_k [\omega^2(\mathrm{LO}k) - \omega^2(\mathrm{TO}j)]\Big/\prod_{k\neq j}[\omega^2(\mathrm{TO}k) - \omega^2(\mathrm{TO}j)]. \tag{2}$$

The temperature dependence of the oscillator strengths is given in figure 7. A large increase in the strength S_1 is shown above 400 °C for both A_1 and E phonons while the strength S_2 of the second mode is nearly constant in the whole temperature range. Finally, the strength S_3 of the TO3 phonon found to be equal to 2 is not given in the figure.

Now we analyse the Raman data in the light of the dielectric measurements, the lattice dynamics calculations and the results of spontaneous polarization successively.

3.2. Dielectric behaviour

The dielectric permittivity along the tetragonal a and c axes are calculated from the values of the oscillator strengths (equation (2)) via the sum rule

$$\varepsilon_\alpha = \sum_j S_{j,\alpha} + \varepsilon_\alpha(\infty) \tag{3}$$

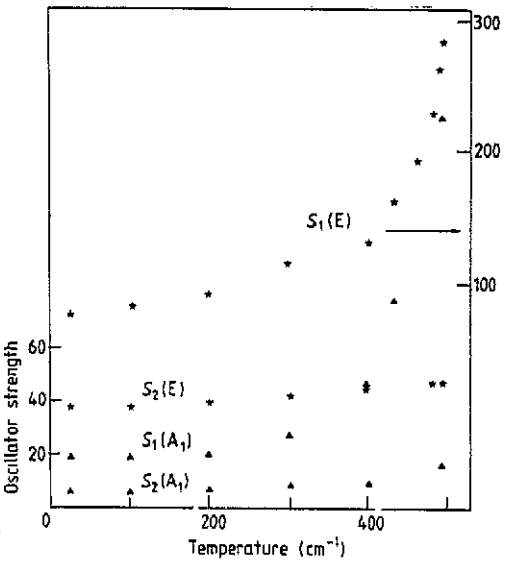

Figure 7. Temperature dependence of the oscillator strengths for the TO1 and TO2 phonons of A_1 (▲) and E (★) symmetry. The strength S_3 of the TO3 phonon is found to be equal to 2 in the whole temperature range.

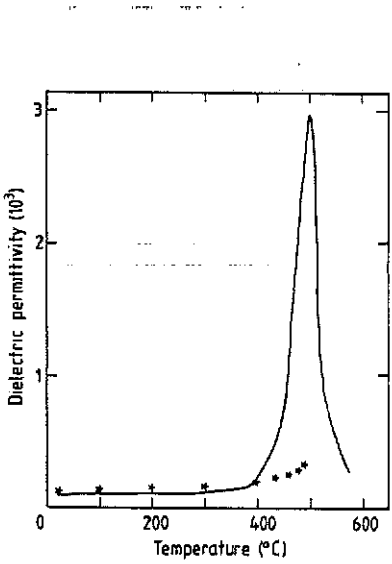

Figure 8. Temperature dependence of the dielectric permittivity along the tetragonal a axis in $PbTiO_3$. The experimental data obtained at 1 MHz (———) are compared with the calculated values (★) derived from equation (3) which involve ionic and electronic contributions.

where $\alpha = a, c$ and $\varepsilon(\infty)$ is the high-frequency dielectric permittivity taken as the square of the optical refractive index [14]. These calculated values of ε, denoted ε(calc), thus involve contributions issued from ionic and electronic resonances. If they are compared with the results directly measured at 1 MHz, fairly good agreement is obtained at room temperature for both directions. Thus we find that ε_a(calc) = 130 compared with ε_a(exp) = 100 and ε_c(calc) = 35 compared with ε_c(exp) = 32.

This is indicative that no additional excitation takes place in the dielectric response between the frequency of the dielectric data and the soft-phonon resonance as long as the temperature is far away from T_c. On the contrary, whereas ε_c(calc) reproduces the increase in ε_c(exp) with increasing temperature, a large discrepancy is revealed in figure 8 above 450 °C between the values of ε_a(calc) and ε_a(exp). This is in agreement with the existence of the quasi-elastic scattering detected in the E spectrum below the soft phonon. In a previous paper, we have shown that this scattering can be described by a Debye relaxation mode uncoupled with soft phonon [15]. If the value ε_a is calculated in the strength associated with this additional mode, complete agreement can be achieved with the experimental data ε_a(exp) for each temperature.

3.3. Lattice dynamics considerations

Lattice dynamical calculations were made for the tetragonal and cubic phases of $PbTiO_3$ [16] by means of a shell model similar to that used for cubic $SrTiO_3$ [17]. Phonon softening was found to be attributed to a change in the short-range interaction between lead and oxygen ions along this bond. Further, the oxygen polarizability displays

values much smaller than those for the isomorphous $BaTiO_3$ and therefore does not play a dominant role in the dynamical behaviour, contrary to many oxidic perovskites. This probably explains the weak intensity of the second-order Raman processes found for $PbTiO_3$. In addition to phonon frequencies for various symmetries, our calculations provide the phonon eigenvectors for each wavevector. In the zero-wavevector limit the soft TO1 phonon is found to correspond to a large vibration of the lead ion with respect to a TiO_6 group which is only slightly distorted. The second TO2 phonon consists of a displacement of the Ti ion and oxygen ions in opposite directions. This kind of ionic vibration corresponds to the soft phonon in $BaTiO_3$ and in most oxidic perovskites.

The inversion of the atomic displacement pattern associated with the TO1 and TO2 phonons in the case of $PbTiO_3$ compared with other ABO_3 compounds can explain the special Raman lineshape, and in particular the fact that the TO1 and TO2 lines have nearly the same intensities.

3.4. Calculation of the effective charges and the spontaneous polarization

Ionic effective charges provide information about the chemical ionic bonding. The temperature dependence of charges thus allows us to study the chemical change connected with a phase transition. The effective charges Z are defined from the following equation [18]:

$$\frac{1}{v}\sum_{\kappa}\frac{(z_\kappa e)^2_\alpha}{m_\kappa} = \varepsilon_v(2\pi c)^2\sum_j(\omega^2_{LOj}-\omega^2_{TOj})_\alpha \tag{4}$$

where the TO and TO phonon frequencies are given in reciprocal centimetres; ε_v is the vacuum dielectric constant, e is the elementary electric charge, c is the velocity of light, m_κ is the mass of the κth ion and v is the unit cell volume. The left-hand summation is made on all the ions κ included in the unit cell whereas the right-hand sum is over all infrared-active modes. In equation (4) the index α denotes the polarization direction of the phonon so that the charge can display a value different according to the direction. We therefore distinguish for each ion the charge $Z_\parallel$ along the tetragonal c axis and the charge $Z_\perp$ along the tetragonal a axis.

In addition to equation (4) the condition of the unit-cell electrical neutrality

$$Z(\mathrm{Pb}) + Z(\mathrm{Ti}) + 3Z(\mathrm{O}) = 0 \tag{5}$$

is involved in the calculations of the ionic effective charges. However, an assumption concerning one of the three charges is needed. Thus we fix the value Z(Ti) and we determine Z(Pb) and Z(O) from equations (4) and (5). The value Z(Ti) = 2.8 is found to be an acceptable value for the reasons mentioned below.

The values Z(Pb) and Z(O) are calculated along the a and c axes as a function of temperature from the phonon frequencies of the E and A_1 symmetries, respectively. The results are illustrated in figure 9. Z(O) as Z(Pb) are largely anisotropic at room temperature. Thus Z(Pb) varies for nearly three orders of magnitude between the directions parallel and normal to the ferroelectric axis. The very low value of the effective charge $Z_\parallel$(Pb) (compared with the nominal value of +2) is indicative of mainly covalent bonds along the c axis.

As the temperature increases, the anisotropy continuously decreases for both Z(O) and Z(Pb). It is remarkable to find nearly isotropic values just below the transition to the cubic phase. In fact the behaviours of the effective charges along the c and a axes

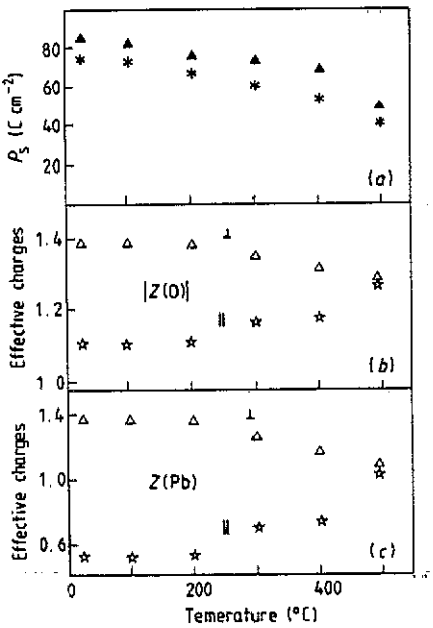

Figure 9. Temperature dependences of (*b*) the effective charge of oxygen ions and (*c*) the effective charge of lead ions along the *c* (‖) and *a* (⊥) axes, together with (*a*) the temperature dependence of spontaneous polarization, as determined experimentally [20] (*) and calculated from equation (6) (▲).

reflect the temperature dependence of the lattice parameters *c* and *a*. Since effective charges are calculated from phonon frequencies only, this proves that the phonon dynamics are mainly governed by the short-range interactions which depend on the interatomic distances.

The spontaneous polarization can be calculated from the values of effective charges as

$$P_s = \frac{e}{v} \sum_{\kappa} \varepsilon_{\parallel}(\infty)^{1/2} Z_{\parallel}(\kappa) \delta(\kappa) \tag{6}$$

where $\delta(\kappa)$ is the spontaneous displacement of the ion κ from the cubic position. The temperature dependence of P_s is thus determined from the values of the effective charges along the *c* axis, the ionic displacements [19] and the optical refractive index [14]. The results are shown in figure 9. At room temperature the value of P_s is found to be equal to 85 C cm^{-2} and then to decrease on heating. The calculated P_s is in relative good agreement with experimental data of Gavrilyachenko *et al* [20].

The accordance which is achieved between experimental and calculated values of the spontaneous polarization proves the relative validity of the values of the effective ionic charges which are found, despite the assumptions mentioned above.

4. Conclusion

Light scattering data in tetragonal and cubic $PbTiO_3$ reveal several features which are connected either to the lattice vibrational modes or to a disorder process. Thus, while the dielectric properties are mainly governed by a relaxation mode around T_c, the spontaneous polarization behaviour is shown to be due to a change in the ionic bonds caused by phonon dynamics, and in particular the soft phonon. Whereas the displacive picture governs all properties below 430 °C, the order–disorder process becomes increasingly efficient when T_c is approached. In fact, both phenomena as revealed in the Raman

spectra are closely related to each other. Thus, if the changes in the slope of the temperature behaviour of several characteristics such ω_{TO1}, γ_{TO1} and P_s are considered, they are seemingly affected by the increasing ionic disorder above 430 °C.

The relaxation process which displays a critical slowing down when T_c is approached from below and from above [15] is consequently interpreted to be the driving mechanism of the cubic-to-tetragonal phase transition in $PbTiO_3$. Several features derived from other techniques support this view. Indeed the deviation of the refractive index from the linear temperature dependence in the cubic phase [14] as well as the ionic displacements emerging from neutron diffraction data [21] indicate the existence of ionic disorder in the cubic $PbTiO_3$ lattice. Likewise, the very recent measurement of electric field gradients [22] in tetragonal $PbTiO_3$ support an order–disorder description of the phase transition in $PbTiO_3$. Finally the Raman spectra reported for various particle sizes of $PbTiO_3$ [23] can also be reanalysed in terms of the coexisting relaxational central peak and soft-phonon line. Indeed when the particle size is very small, the soft-phonon lineshape broadens and the quasi-elastic scattering increases as T_c is approached, so that the low-frequency spectrum consists only of a broad central peak for temperatures close to T_c. If it is compared with our Raman data obtained in the bulk crystal, this change in the profile can be understood as due to enhancing ionic disorder for decreasing lattice size.

References

[1] Scalabrin A, Chaves A S, Shim D S and Porto S P S 1977 *Phys. Status Solidi* b **79** 731
Luspin Y, Servoin J L and Gervais F 1980 *J. Phys. C: Solid State Phys.* **13** 3761
[2] Fontana M D, Métrat G, Servoin J L and Gervais F 1984 *J. Phys. C: Solid State Phys.* **174** 83
[3] Fontana M D, Ridah A, Kugel G E and Carabatos-Nedelec C 1988 *J. Phys. C: Solid State Phys.* **21** 5853
[4] Maglione M, Bohmer R, Loidl A and Höchli U T 1989 *Physica* B **40** 11441
[5] Kania A, Roleder K, Kugel G E and Fontana M D 1986 *J. Phys. C: Solid State Phys.* **19** 9
[6] Roleder K, Kugel G E and Fontana M D 1990 *Ferroelectrics* **112** 225
[7] Okamoto Y, Wang P and Scott J F 1985 *Phys. Rev.* B **32** 6787
Zhang M and Scott J F 1986 *Phys. Rev.* B **34** 1880
[8] Shirane G, Axe J D, Harada J and Remeika J P 1970 *Phys. Rev.* B **2** 155
[9] Burns G and Scott B A 1973 *Phys. Rev.* B **7** 3088
[10] Frey R A and Silberman E 1976 *Helv. Phys. Acta* **49** 1
[11] Kobayashi J, Uesu Y, Sakemi Y and Mokokawa T 1980 *Phys. Status Solidi* a **59** K143
Kobayashi J, Uesu Y and Sakemi Y 1983 *Phys. Rev.* B **28** 3866
[12] Migoni R, Bilz H and Bauerle D 1976 *Phys. Rev. Lett.* **37** 1155
Kugel G E, Mesli H and Fontana M D 1988 *Phys. Rev.* B **37** 5619
[13] Wojcik K 1988 *Ferroelectrics* **82** 25
[14] Kleemann W, Schäfer F J and Rytz D 1986 *Phys. Rev.* B **34** 7873
[15] Fontana M D, Idrissi H and Wojcik K 1990 *Europhys. Lett.* **11** 419
[16] Fontana M D, Idrissi H and Carabatos-Nedelec C 1990 *Phonons '89* (Singapore: World Scientific) p 1135
[17] Cowley R A 1964 *Phys. Rev.* **134** 1981
Stirling W G 1972 *J. Phys. C: Solid State Phys.* **5** 2711
[18] Scott J F 1971 *Phys. Rev.* B **4** 1360
Gervais F and Arend H 1983 *Z. Phys.* B **50** 17
[19] Glazer A M and Mabud S A 1978 *Acta Crystallogr.* B **34** 1065
Nelmes R J and Kuhs W F 1985 *Solid State Commun.* **54** 721
[20] Gavrilyachenko V G, Spinko R I, Martynenko M A and Fesenko E G 1970 *Sov. Phys.–Solid State* **12** 1203
[21] Nelmes R J, Piltz R O, Kuhs W F, Tun Z and Restori R 1990 *Ferroelectrics* **108** 1771
[22] Catchen G L, Wukitch S J, Spaar D M and Blazkiewicz M 1990 *Phys. Rev.* B **42** 1885
[23] Ishikawa K, Yoshikawa K and Okada N 1988 *Phys. Rev.* B **37** 5852